# Nominal Trajectories of an autonomous under-actuated airship

Yasmina Bestaoui

# Nominal Trajectories of an Autonomous Under-actuated Airship

**Yasmina Bestaoui**

**Abstract:** The objective of this paper is to generate a desired flight path to be followed by an autonomous airship. The space is supposed without obstacles. As there are six degrees of freedom and only three inputs for the LSC AS200 airship, three equality constraints appear due to the under-actuation.

**Keywords:** Autonomous airship, trajectory generation, under-actuation.

## 1. INTRODUCTION

Lighter than air vehicles suit a wide range of applications, ranging from advertising, aerial photography and aerial inspection platforms, with a very important application in the areas of environmental, biodiversity, and climatological research and monitoring. Airships offer the advantage of quiet hover with noise levels much lower than helicopters. Unmanned remotely-operated airships have already proved themselves as camera and TV platforms and for specialized scientific tasks. An actual trend is toward autonomous airships.

Fig. 1 presents the AS200 airship. It is basically a large gas balloon. Its shape is maintained by its internal overpressure. The only solid parts are the gondola, a tail rotor with horizontal axis of rotation, the main rotor with a varying tilt angle and the tail fins. It is actually a remotely piloted airship designed for remote sensing, being transformed to be fully autonomous.

A basic problem to be solved by autonomous vehicles is the problem of trajectory generation. Trajectory generation means the generation and execution of a plan for moving from one location to another location in space to accomplish a desired task. The motion generation module generates a nominal state space trajectory and a nominal control input. Trajectory prediction consists in computing reference values to be given to the controller.

The problem of finding the time-optimal trajectory for a fully actuated robot manipulator along a specified path is a classical one in robotics. This problem has been solved by algorithms proposed by [1-5]. The algorithms find the minimum time scaling of the path with respect to the actuator constraints: dynamic ones [1,4] and technological ones [2,6]. The problem of finding a smooth interpolating curve is well understood in Euclidean spaces, but it is not so clear in curved spaces [7]. When planning Cartesian trajectories, it is usually possible to characterize the performance of different trajectories [2,4,6,7-17].

In [18], in the first part, the trajectories considered are trim trajectories. The general condition for trim requires that the rate of change of the magnitude of the velocity vector is identically zero, in the body fixed frame. The trim problem is generally formulated as a set of non linear algebraic equations. The solution trajectories are helices with constant curvature and torsion. In the second part, variable curvature helices are investigated. In [9], a 3rd order expansion is used for transition maneuvering between two helices. [19] investigate optimal trajectory planning for hot air balloons in linear wind fields. The objective function to be minimized is fuel consumption with respect to free end states.

This article is concerned with methods of computing a trajectory in space that describes the desired motion. The contribution of this paper is the characterization of trajectories, considering the under-actuation. This paper consists of 6 sections. Section 2

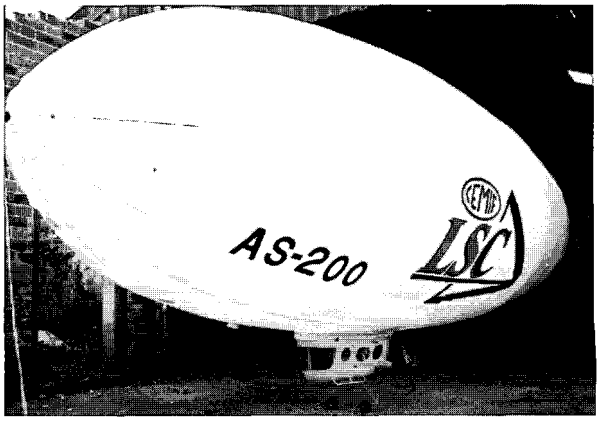


Fig. 1. The AS200 airship.

Manuscript received May 11, 2005; revised April 5, 2006; accepted May 10, 2006. Recommended by Editor Keum-Shik Hong.

Yasmina Bestaoui is with the Laboratoire IBISC CNRS FRE2873, University of Evry, 38 rue du Pelvoux, 91025 EVRY, France (e-mail: bestaoui@iup.univ-evry.fr).

presents the kinematics while the following one introduces the mechanical system. Section 4 introduces the relationship between trajectory generation algorithms and under-actuation. Simulation results are discussed in Section 5 and finally some concluding remarks are given in section 6.

## 2. KINEMATICS

Consider a rigid body moving in free space. Assume any inertial reference frame {F} fixed in space and a frame {M} fixed to the body at the center of gravity. At each instant, the configuration (position and orientation) of the rigid body can be described by a homogeneous transformation matrix corresponding to the displacement from frame {F}to frame {M}.

The origin C of {M} coincides with the center of gravity of the vehicle. Its axes ($X_c$ $Y_c$ $Z_c$) are the principal axes of symmetry when available. They must form a right handed orthogonal normed frame. The position of the vehicle C in {F} can be described by $\eta_1 = (x\ y\ z)^T$ while the orientation is given by $\eta_2 = (\phi\ \theta\ \psi)^T$ with $\phi$ Roll, $\theta$ pitch and $\psi$ Yaw angles. The orientation matrix R is given by

$$R = \begin{pmatrix} c\psi c\theta & -s\psi c\phi + c\psi s\theta s\phi & s\psi s\phi + c\psi s\theta c\phi \\ s\psi c\theta & c\psi c\phi + s\psi s\theta s\phi & -c\psi s\phi + s\psi s\theta c\phi \\ -s\theta & c\theta s\phi & c\theta c\phi \end{pmatrix}, \quad (1)$$

where $c\theta = \cos(\theta)$ and $s\theta = \sin(\theta)$. This description is valid in the region $-\frac{\pi}{2} < \theta < \frac{\pi}{2}$. A singularity of this transformation exists for: $\theta = \frac{\pi}{2} \pm k\pi,\ k \in Z$.

The kinematics of the airship can be expressed in the following way:

$$\begin{pmatrix} \dot{\eta}_1 \\ \dot{\eta}_2 \end{pmatrix} = \begin{pmatrix} R & 0_{3*3} \\ 0_{3*3} & J\ (\eta_2) \end{pmatrix} \begin{pmatrix} V \\ \Omega \end{pmatrix}, \quad (2)$$

where

$$J\ (\eta_2) = \begin{pmatrix} 1 & s\phi.\tan\theta & c\phi.\tan\theta \\ 0 & c\phi. & -s\phi \\ 0 & s\phi/c\theta & c\phi/c\theta \end{pmatrix}, \quad (3)$$

and

$$V = \begin{pmatrix} u \\ v \\ w \end{pmatrix}, \quad \omega = \begin{pmatrix} p \\ q \\ r \end{pmatrix}. \quad (4)$$

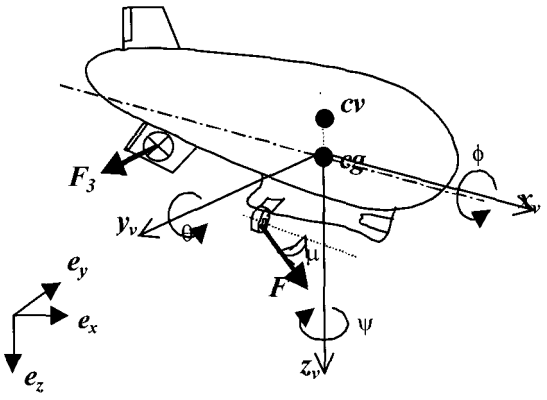


Fig. 2. The airship frames (cg: center of gravity, cv: center of volume).

$\omega$ physically corresponds to the angular velocity of the rigid body, while $V$ is the linear velocity of the origin C of the frame {M}.

## 3. MECHANICAL SYSTEM

3.1. Dynamics

In this section, analytic expressions for the forces and moments of a system with added mass and inertia such as an airship are introduced [5,20-22]. An airship is a lighter than air vehicle using a lifting gas (helium in this particular case). We will make in the sequel some simplifying assumptions: the earth fixed frame is inertial, the gravitational field is constant, the airship is well inflated, the density of air is uniform. In [23], we considered the case of an airship with small deformations analyzed via the Updated Lagrangian Method.

The translational part being separated from the rotational part [20], the dynamic equations (Euler – Poincaré) are given by:

$$\begin{aligned} M\dot{V} &= -\omega * MV - b(.) + f(u), \\ J\dot{\omega} &= -\omega * J\omega - V * MV - \beta(.) + \tau(u), \end{aligned} \quad (5)$$

where

$$b(.) = R^T e_3 (mg - B) + D_V V, \quad (6)$$

$$\beta(.) = (R^T e_3 * \overline{BG})B + D_\omega \omega. \quad (7)$$

For a system with added masses, the term $V * MV$ is non zero. $M$ and $J$ are respectively the vehicle's mass and rotational tensors and $\tau$, $\beta$ and f, b represent respectively the control and non-conservative torques and forces in body axes. m is the mass of the airship, propellers and actuators. The tensor M includes both the airship's actual mass as well as the virtual mass elements associated with the dynamics of buoyant vehicles. The tensor J includes both the airship's

actual inertias as well as the virtual inertia elements associated with the dynamics of buoyant vehicles. As the airship displays a very large volume, its added masses and inertias become very significant [21]. We will assume that the added mass coefficients are constant. They can be estimated from the inertia ratios and the airship weight and dimension parameters. Added mass should be understood as pressure-induced forces and moments due to a harmonic motion of the body which are proportional to the acceleration of the body [21]. $D_V$ is the 3×3 aerodynamics forces diagonal matrix while $D_\Omega$ is the 3×3 aerodynamics moments diagonal matrix. $e_3 = (0\ 0\ 1)^T$ a unit vector.

The 3×1 buoyancy force vector $Be_3$ with:

$$B = \rho \Delta g, \tag{8}$$

where $\Delta$ is the volume of the envelope, $\rho$ is the difference between the density of the ambient atmosphere $\rho_{air}$ and the density of the helium $\rho_{helium}$ in the envelope, g is the constant gravity acceleration.

$\overrightarrow{BG} = \begin{pmatrix} x_b & y_b & z_b \end{pmatrix}$ represents the position of the center of buoyancy with respect to the body fixed frame.

The aerodynamic force can be resolved into two component forces, one parallel and the other perpendicular to the direction of motion. Lift is the component of the aerodynamic force perpendicular to the direction of motion and drag is the component opposite to the direction of motion. As the airship is a slow moving object in the air, we can assume a linear relationship between the speed and the drag.

$$D_V = diag\begin{pmatrix} -X_u & -Y_v & -Z_w \end{pmatrix}, \tag{9}$$

$$D_\Omega = diag\begin{pmatrix} -L_p & -M_q & -N_r \end{pmatrix}. \tag{10}$$

The gravitational force vector is given by the difference between the airship weight and the buoyancy acting upwards on it:

$$R^T e_3 (mg - B) = \begin{pmatrix} (mg - B)s\theta \\ -(mg - B)c\theta.s\phi \\ -(mg - B)c\theta.c\phi \end{pmatrix}. \tag{11}$$

The gravitational and buoyant moments are given by:

$$\left( R^T e_3 * \overrightarrow{BG} \right) B = B \begin{pmatrix} z_b c\theta s\phi - y_b c\theta c\phi \\ x_b c\theta c\phi + z_b s\theta \\ -y_b s\theta - x_b c\theta s\phi \end{pmatrix}. \tag{12}$$

If a system is fully actuated, it can be steered along any given curve on the configuration manifold, i.e it is controllable. This is not true in general for an under-actuated system. However, an under-actuated system can be locally controllable if it enjoys the property of nonholonomy. The existence of nonholonomic constraints translates into the fact that the system can be locally steered along a manifold of dimension larger than the number of independent control inputs [3,13-15,18,21]. However, practical methods have only been found for simple underactuated systems.

3.2. Propulsion

An airship is propelled by thrust. Propellers are designed to exert thrust to drive the airship forward. The most popular propulsion system layout for pressurized non rigid airships is twin ducted propellers mounted either side of the envelope bottom. Another one exists in the tail for torque correction and attitude control. The airship AS200 is an under-actuated system with two types of control in a low velocity flight: forces generated by thrusters and angular inputs controlling the direction of the thrusters ( $\gamma$ is the tilt angle of the propellers)

$$F_1 = \begin{pmatrix} T_M \sin\gamma \\ 0 \\ T_M \cos\gamma \end{pmatrix}, \quad F_2 = \begin{pmatrix} 0 \\ T_T \\ 0 \end{pmatrix}, \tag{13}$$

where $T_M$ and $T_T$ represent respectively the main and tail thrusters.

Thus in building the non linear six degrees of freedom mathematical model, the additional following assumptions are made:

$$\overrightarrow{P_1G} = \begin{pmatrix} 0 \\ 0 \\ P_1^3 \end{pmatrix}, \quad \overrightarrow{P_2G} = \begin{pmatrix} P_2^1 \\ 0 \\ 0 \end{pmatrix}. \tag{14}$$

If we consider the plane XZ as a plane of symmetry, the mass and inertia matrices can be written as:

$$M = \begin{pmatrix} m + X_u & 0 & X_z \\ 0 & m + Y_v & 0 \\ Z_x & 0 & m + Z_w \end{pmatrix}, \tag{15}$$

$$J = \begin{pmatrix} I_x + L_p & 0 & -I_{xz} \\ 0 & I_y + M_q & 0 \\ -I_{xz} & 0 & I_z + N_r \end{pmatrix}. \tag{16}$$

If the center of gravity sits below the center of buoyancy, then $\overrightarrow{BG} = \begin{pmatrix} 0 & 0 & z_b \end{pmatrix}^T$. It is important to gain insight into the geometric structure of the equations since this knowledge is useful in motion planning and control.

## 4. TRAJECTORY GENERATION AND UNDERACTUATION

In this paragraph, nominal trajectories are characterized, the model is supposed perfect and any

perturbation such as wind or sensor disturbance is neglected. The three equality constraints deriving from the under-actuation are sought. Considering the dynamics of the airship and its propulsion, the following dynamics equations can be written:

$$f(u) = M\dot{V} + \omega * MV + b(.) = \begin{pmatrix} T_M \sin\gamma \\ T_T \\ T_M \cos\gamma \end{pmatrix}, \qquad (17)$$

$$\tau(u) = J\dot{\omega} + \omega * J\omega + V * MV + \beta(.) = \begin{pmatrix} 0 \\ P_1^3 T_M \sin\gamma \\ P_2^1 T_T \end{pmatrix} = \begin{pmatrix} 0 \\ P_1^3 f_1(u) \\ P_2^1 f_2(u) \end{pmatrix}, \qquad (18)$$

where the kinematics are:

$$\begin{aligned} p &= \dot{\phi} - \dot{\psi} S\theta, \\ q &= \dot{\theta} C\phi + \dot{\psi} S\phi C\theta, \\ r &= -\dot{\theta} S\phi + \dot{\psi} C\phi C\theta. \end{aligned} \qquad (19)$$

**First equality constraint:** The roll moment being zero (see (18)), $\tau_1 = 0$ gives

$$\begin{aligned} & J_{11}\left(\ddot{\phi} - \ddot{\psi} S\theta - \dot{\psi}\dot{\theta} C\theta\right) \\ & + (J_{33} - J_{22})\left(\dot{\theta} C\phi + \dot{\psi} S\phi C\theta\right)\left(-\dot{\theta} S\phi + \dot{\psi} C\phi C\theta\right) \\ & + D_p\left(\dot{\phi} - \dot{\psi} S\theta\right) + z_b BC\theta S\phi = 0. \end{aligned} \qquad (20)$$

**Second equality constraint:** $P_1^3 f_1 = \tau_2$ gives

$$\begin{aligned} & J_{22}\chi + (M_{11} - M_{33})uw \\ & + (J_{11} - J_{33})\left(\dot{\phi} - \dot{\psi} S\theta\right)\left(-\dot{\theta} S\phi + \dot{\psi} C\phi C\theta\right) \\ & + D_q\left(\dot{\theta} C\phi + \dot{\psi} S\phi C\theta\right) - z_b BS\theta + P_1^3 M_{11}\dot{u} \\ & + P_1^3 M_{22} w\left(\dot{\theta} C\phi + \dot{\psi} S\phi C\theta\right) \\ & - P_1^3 M_{22} v\left(-\dot{\theta} S\phi + \dot{\psi} C\phi C\theta\right) \\ & + P_1^3 D_u u + P_1^3 (mg - B) S\theta = 0, \end{aligned} \qquad (21)$$

where

$$\chi = \ddot{\theta} C\phi - \dot{\theta}\dot{\phi} S\phi + \ddot{\psi} S\phi C\theta + \dot{\psi}\dot{\phi} C\phi C\theta - \dot{\psi}\dot{\theta} S\phi S\theta.$$

**Third equality constraint:** $P_2^1 f_2 = \tau_3$ gives

$$\begin{aligned} & J_{33}\chi' + (M_{22} - M_{11})uv \\ & + (J_{22} - J_{11})\left(\dot{\phi} - \dot{\psi} S\theta\right)\left(\dot{\theta} C\phi + \dot{\psi} S\phi C\theta\right) \\ & + N_r\left(-\dot{\theta} S\phi + \dot{\psi} C\phi C\theta\right) + P_1^2 M_{22}\dot{v} \\ & - P_1^2 M_{22} w\left(\dot{\phi} - \dot{\psi} S\theta\right) + P_1^2 M_{11} u\left(-\dot{\theta} S\phi + \dot{\psi} C\phi C\theta\right) \\ & + P_1^2 D_v v - P_1^2 (mg - B) S\phi C\theta = 0, \end{aligned} \qquad (22)$$

where

$$\chi' = -\ddot{\theta} S\phi - \dot{\theta}\dot{\phi} C\phi + \ddot{\psi} C\phi C\theta - \dot{\psi}\dot{\phi} S\phi C\theta - \dot{\psi}\dot{\theta} C\phi S\theta.$$

The following approach is considered. The variations of the roll and pitch angles as well as the longitudinal velocity are imposed and the influence of the under-actuation on the variations of the yaw angle, the lateral and vertical velocities are studied.

The first equality constraint (20) is equivalent to the resolution of an ordinary differential equation of the form

$$a(t)\ddot{\psi} + b(t)\left(\dot{\psi}\right)^2 + c(t)\dot{\psi} + d(t) = 0, \qquad (23)$$

where

$$\begin{aligned} a(t) &= J_{11}(S\theta), \\ b(t) &= (J_{33} - J_{22})\left(C\phi S\phi C^2\theta\right), \\ c(t) &= -S\theta D_p + 2(J_{33} - J_{22}) C\theta C^2\phi \\ &\quad - (J_{11} + J_{33} - J_{22})\dot{\theta} C\theta, \\ d(t) &= -z_b BC\theta S\phi - J_{11}\ddot{\phi} - D_p\dot{\phi} \\ &\quad + (J_{33} - J_{22})\dot{\theta}^2 S\phi C\phi. \end{aligned} \qquad (24)$$

If $\Xi(t) = \dot{\psi}(t)$ then the non autonomous generalized logistic equation must be solved:

$$a(t)\dot{\Xi}(t) + b(t)\left(\Xi(t)\right)^2 + c(t)\Xi(t) + d(t) = 0. \qquad (25)$$

The third equality constraint (22) can be written as:

$$w(t) = \alpha_0 + \alpha_1 u + \alpha_2 v + \alpha_3 uv + \alpha_4\dot{v}, \qquad (26)$$

where

$$\alpha_0 = \frac{\alpha'_0 (J_{22} - J_{11}) - P_1^2 (mg - B) C\theta S\phi + D_r\left(\dot{\psi} C\theta C\phi - \dot{\theta} S\phi\right)}{-P_1^2 M_{22}\left(\dot{\psi} S\theta - \dot{\phi}\right)}$$

$$+\frac{J_{33}\left(\ddot{\psi}C\theta C\phi-\ddot{\theta}S\phi-\dot{\psi}\dot{\theta}S\theta C\phi-\dot{\psi}\dot{\phi}C\theta S\phi-\dot{\theta}\dot{\phi}C\phi\right)}{-P_1^2M_{22}\left(\dot{\psi}S\theta-\dot{\phi}\right)},$$

$$\alpha_1=-\frac{\left(\dot{\psi}C\theta C\phi-\dot{\theta}S\phi\right)M_{11}}{\left(\dot{\psi}S\theta-\dot{\phi}\right)M_{22}},$$

$$\alpha_2=\frac{-D_v}{\left(\dot{\psi}S\theta-\dot{\phi}\right)M_{22}},$$

$$\alpha_3=\frac{M_{11}-M_{22}}{P_1^2M_{22}\left(\dot{\psi}S\theta-\dot{\phi}\right)},$$

$$\alpha_4=\frac{-1}{\left(\dot{\psi}S\theta-\dot{\phi}\right)},$$

(27)

and

$$\alpha'_0=\left(-\dot{\psi}^2S\theta C\theta S\phi-\dot{\psi}\dot{\theta}S\theta C\phi+\dot{\psi}\dot{\phi}C\theta S\phi+\dot{\theta}\dot{\phi}C\phi\right).$$

The second equality constraint (21) gives:

$$\beta_0+\beta_1u+\beta_2u^2+\beta_3uv+\beta_4u^2v+\beta_5u\dot{v}+\beta_6v+\beta_7\dot{v}+\beta_8\dot{u}=0,\tag{28}$$

where

$$\begin{aligned}
&\beta_0=\beta'_0+\beta'_3\alpha_0, && \beta_1=\beta'_1+\alpha_1\beta'_3+\alpha_0\beta'_5,\\
&\beta_2=\beta'_5\alpha_1, && \beta_3=\beta'_5\alpha_2+\alpha_3\beta'_3,\\
&\beta_4=\beta'_5\alpha_3, && \beta_5=\beta'_5\alpha_4,\\
&\beta_6=\beta'_2+\alpha_2\beta'_3, && \beta_7=\alpha_4\beta'_3,\\
&\beta_8=\beta'_4,
\end{aligned}\tag{29}$$

$$\begin{aligned}
\beta'_0&=J_{22}\beta''_0+\left(J_{11}-J_{33}\right)\beta'''_0\\
&\quad+D_q\left(\dot{\psi}C\theta S\phi+\dot{\theta}C\phi\right)\\
&\quad-Bz_bS\theta+P_1^3\left(mg-B\right)S\theta,\\
\beta''_0&=\ddot{\psi}C\theta S\phi+\ddot{\theta}C\phi+\dot{\psi}\dot{\phi}C\theta C\phi\\
&\quad-\dot{\psi}\dot{\theta}S\theta S\phi-\dot{\theta}\dot{\phi}S\phi,\\
\beta'''_0&=-\dot{\theta}\dot{\phi}S\phi+\dot{\psi}\dot{\phi}C\phi C\theta\\
&\quad+\dot{\psi}\dot{\theta}S\theta S\phi-\dot{\psi}^2C\phi C\theta S\theta,
\end{aligned}$$

$$\begin{aligned}
&\beta'_1=P_1^3X_u,\\
&\beta'_2=-P_1^3M_{22}\left(\dot{\psi}C\theta C\phi-\dot{\theta}S\phi\right),\\
&\beta'_3=P_1^3M_{22}\left(\dot{\psi}C\theta S\phi+\dot{\theta}C\phi\right),\\
&\beta'_4=P_1^3M_{11},\\
&\beta'_5=\left(M_{11}-M_{22}\right).
\end{aligned}$$

4.1. Roll and pitch angles constant

The differential equation

$$a\ddot{\psi}+b\left(\dot{\psi}\right)^2+c\dot{\psi}+d=0,\tag{30}$$

where

$$\begin{aligned}
&a=-J_{11}\left(S\theta\right),\\
&b=\left(J_{33}-J_{22}\right)\left(S\phi C\theta\right)\left(C\phi C\theta\right),\\
&c=D_p\left(-S\theta\right),\\
&d=-z_bBC\theta S\phi
\end{aligned}\tag{31}$$

admits an analytic general solution.

By using the method of separation of variables and integration by partial fractions, in the constant coefficient case, logistic equation can be solved and the behavior of all solutions is analyzed [24-27].

For $\phi=0$;

$$\psi(t)=\psi_0e^{-L_pt/I_x}.\tag{32}$$

For $\theta=0$;

$$\psi\left(t\right)=t\sqrt{\frac{Bz_b}{C\phi\left(I_z-I_y\right)}}+\psi_0.\tag{33}$$

For the particular case, where $\dot{\psi}$ is constant, classical trim trajectories are encountered.

4.1.1 $\dot{\psi}$ is constant:

$$\begin{pmatrix}\phi=cst=\phi_0\\ \theta=cst=\theta_0\\ \psi=\dot{\psi}_0t\end{pmatrix}.\tag{34}$$

The first equality constraint becomes a second order polynomial equation:

$$b\left(\dot{\psi}\right)^2+c\dot{\psi}+d=0.\tag{35}$$

The third equality constraint gives

$$w(t) = \alpha_0 + \alpha_1 u + \alpha_2 v + \alpha_3 uv + \alpha_4 \dot{v}, \tag{36}$$

where

$$\begin{aligned}
\alpha_0 &= \frac{-\dot{\psi}^2 S\theta C\theta S\phi (J_{22} - J_{11}) + D_r \dot{\psi} C\theta C\phi}{P_1^2 \dot{\psi} S\theta M_{22}} \\
&\quad + \frac{-P_1^2 (mb - B) C\theta S\phi + J_{33} \ddot{\psi} C\theta C\phi}{P_1^2 \dot{\psi} S\theta M_{22}}, \\
\alpha_1 &= -\frac{C\theta C\phi M_{11}}{S\theta M_{22}}, \\
\alpha_2 &= \frac{D_v}{M_{22} \dot{\psi} S\theta}, \\
\alpha_3 &= \frac{M_{11} - M_{22}}{P_1^2 M_{22} \dot{\psi} S\theta}, \\
\alpha_4 &= \frac{1}{\dot{\psi} S\theta},
\end{aligned} \tag{37}$$

while the second equality constraint gives

$$v = -\frac{\beta_0 + \beta_1 u + \beta_2 u^2}{\beta_6 + \beta_3 u + \beta_4 u^2} \tag{38}$$

for $\dot{u} = \dot{v} = 0$,
otherwise

$$\begin{aligned}
&\beta_0 + \beta_1 u + \beta_2 u^2 + \beta_3 uv + \beta_4 u^2 v + \beta_5 u \dot{v} \\
&+ \beta_6 v + \beta_7 \dot{v} + \beta_8 \dot{u} = 0
\end{aligned} \tag{39}$$

with the parameters $\beta_i$ given in (29)-(31).

When $\dot{u} = \dot{v} = \dot{w} = 0$, we retrieve the classical kinematics equations of the trim trajectories

$$\begin{aligned}
\dot{x} &= a_x \cos(\dot{\psi}_0 t) + b_x \sin(\dot{\psi}_0 t), \\
\dot{y} &= a_y \cos(\dot{\psi}_0 t) + b_y \sin(\dot{\psi}_0 t), \\
\dot{z} &= -\sin(\theta_0) u_0 + \cos(\theta_0) \sin(\phi_0) v_0 + \cos(\theta_0) \cos(\phi_0) w_0,
\end{aligned} \tag{40}$$

where

$$\begin{aligned}
a_x &= \cos(\theta_0) u_0 + \sin(\theta_0) \sin(\phi_0) v_0 + \sin(\theta_0) \cos(\phi_0) w_0, \\
b_y &= a_x, \\
b_x &= -\cos(\phi_0) v_0 + \sin(\phi_0) w_0, \\
a_y &= -b_x.
\end{aligned} \tag{41}$$

Integrating these equations, we obtain

$$\begin{aligned}
x &= \frac{a_x}{\dot{\psi}_0} \sin(\frac{\dot{\psi}_0}{V_e} s) - \frac{b_x}{\dot{\psi}_0} \cos(\frac{\dot{\psi}_0}{V_e} s), \\
y &= -\frac{b_x}{\dot{\psi}_0} \sin(\frac{\dot{\psi}_0}{V_e} s) - \frac{a_x}{\dot{\psi}_0} \cos(\frac{\dot{\psi}_0}{V_e} s), \\
z &= \frac{\dot{z}}{V_e} s,
\end{aligned} \tag{42}$$

where s represents the curvilinear abscissa and we suppose a uniform motion such that

$$s = V_e t = t\sqrt{u_0^2 + v_0^2 + w_0^2}. \tag{43}$$

The trajectories represented by these equations (44) are classical helices rotated around the vertical axe by an angle of $arctan\left(\frac{b_x}{a_x}\right)$ and have a constant curvature and torsion

$$k = \frac{V^2 \sqrt{A_x^2 + B_x^2}}{\sqrt{V^2 \left(A_x^2 + B_x^2\right) + C_x^2}}, \tag{44}$$

$$\tau = \frac{C_x V}{\sqrt{V^2 \left(A_x^2 + B_x^2\right) + C_x^2}}, \tag{45}$$

where

$$A_x = \frac{a_x}{\dot{\psi}_0}, \quad B_x = \frac{b_x}{\dot{\psi}_0}, \tag{46}$$

$$C_x = \frac{\dot{z}_0}{V_e}, \quad V = \frac{\dot{\psi}_0}{V_e}. \tag{47}$$

The trajectory is shown in Fig. 3.

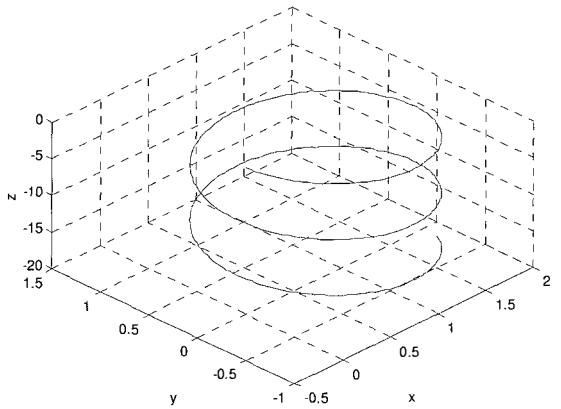


Fig. 3. Trim trajectory.

The trim condition can be a turning (about the vertical axis), descending or climbing (assuming constant air density and temperature), side-slipping maneuver at constant speed. More conventional flight conditions such as hover, cruise, auto-rotation or sustained turns are also trims.

4.1.2 $\dot{\psi}$ is not constant:

Fig. 4 shows the solution $\psi(t)$ of the differential in (20) while Fig. 5 shows its derivative $\dot{\psi}(t)$.
Even though there is a nonlinear variation of $\psi$ in the beginning of the simulation, the yaw angle has a quasilinear variation after a certain time.
A transitional behavior can be recognized before the yaw velocity attains a permanent (constant) value.

4.2. Roll and pitch angles linear functions of time

In this paragraph, the roll and pitch angles are assumed to have linear variations:

$$\theta = \dot{\theta}_0 t + \theta_0, \qquad \phi = \dot{\phi}_0 t + \phi_0.$$

When the coefficients of the non autonomous logistic equation are no longer constant, no explicit solutions can be found in general and the equilibrium point may become unstable [24]. For a study to be complete, the existence of stable periodic or stable bounded solutions is an essential part of qualitative theory of this differential equation, in order to determine non trivial solutions and study their behavior [24-27]. Nkashama [27] proved that the logistic equation with positive non autonomous bounded coefficients has exactly one bounded solutions that is positive and does not tend to the zero solution.

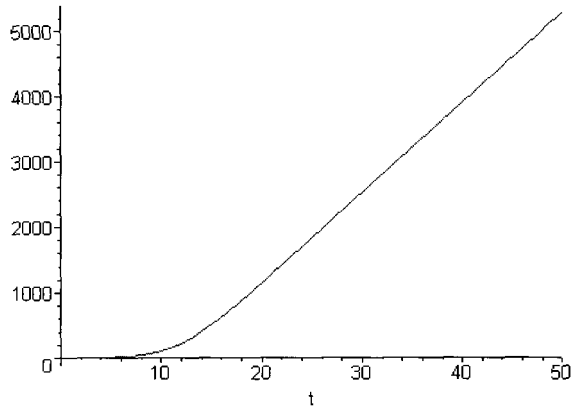

Fig. 4. Yaw angle.

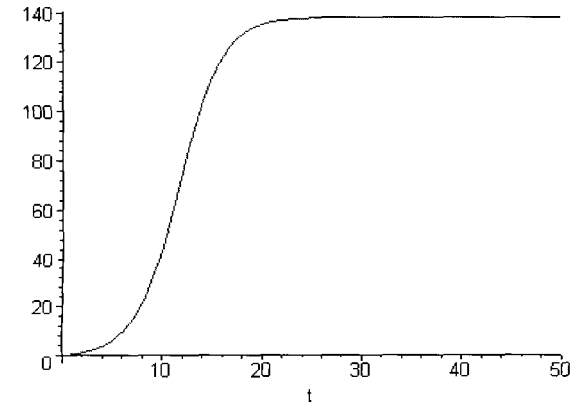

Fig. 5. Yaw derivative.

Solving the first equality constraint, the roll moment being null, $\forall t$, implies $L_p \dot{\phi}_0 = 0 \Rightarrow \dot{\phi}_0 = 0$. Rearranging the first equality constraint with this requirement gives: $\dot{\theta}_0 C\phi_0 S\phi_0 = 0$, three cases are possible

$$\dot{\theta}_0 = 0 \quad or \quad \phi_0 = 0 \quad or \quad \phi_0 = \frac{\pi}{2}.$$

The first case: trim trajectories has already been studied in paragraph 4.1.1.
If the roll angle is null, the following differential equations must be solved:

$$\ddot{\psi} + \dot{\psi}\left(a + b\dot{\theta}_0 C\theta / S\theta\right) = 0,$$

where $a = L_p/(I_x)$,

$$b = -\left(I_z - I_y - I_z\right)/(I_x), \tag{48}$$

the following derivative $\dot{\psi}(t)$ is obtained

$$\dot{\psi}(t) = -\frac{\dot{\theta}_0 S\theta_0{}^b S\theta^{-b} e^{-\frac{a\theta}{\dot{\theta}_0}}}{-\cosh\left(\frac{a\theta_0}{\dot{\theta}_0}\right) + \sinh\left(\frac{a\theta_0}{\dot{\theta}_0}\right)}. \tag{49}$$

The case $\phi_0 = \frac{\pi}{2}$ gives the following differential equations

$$\ddot{\psi} + \dot{\psi}\left(a_1 + a_2\dot{\theta}_0 C\theta / S\theta\right) + a_3 C\theta / S\theta = 0,$$

where $a_1 = L_p/(I_x)$,

$$a_2 = \left(I_z - I_y + I_z\right)/(I_x), \tag{50}$$

$$a_3 = Bz_b / I_x.$$

The third equality constraint gives

$$w = \delta_1 + \delta_2 uv + \delta_3 u + \delta_4 v + \delta_5 \dot{u}. \tag{51}$$

where

$$\delta_1 = \dot{\theta}_0 \frac{I_y + I_z - I_x}{P_2^1 M_y} - \frac{N_r C\theta}{P_2^1 S\theta M_y} - \frac{I_z \ddot{\psi} C\theta}{P_2^1 \dot{\psi} S\theta M_y},$$

$$\delta_2 = -\frac{M_y - M_x}{P_2^1 \dot{\psi} S\theta M_y},$$

$$\delta_3 = -\frac{C\theta M_y}{S\theta M_y},$$

$$\delta_4 = -\frac{Y_v}{\dot{\psi} S\theta M_y},$$

$$\delta_5 = -\frac{1}{\dot{\psi} S\theta}. \qquad (52)$$

Once the yaw angle is calculated, the linear and angular velocities are determined as well as the 3D path.

## 5. SIMULATION RESULTS

The lighter than air platform is the AS200 by Airspeed Airships. It is a remotely piloted airship designed for remote sensing. It is a non rigid 6m long, 1.4m diameter and 8.6m$^3$ volume airship equipped with two vectorable engines on the sides of the gondola and 4 control surfaces at the stern. Envelope pressure is maintained by air fed from the propellers into the two ballonets located inside the central portion of the hull. These ballonets are self regulating and can be fed from either engine. The engines are standard model aircraft type units. The propellers can be rotated through 120 degrees. During flight the rudders and elevators are used for all movements in pitch and yaw.

In Table 1, five cases are presented for a normalized simulation time = 1. For each case, four subplots are presented: the first one presents the trajectory in space, the second one the variation of the yaw angle $\psi$, the linear velocities $v$ and $w$ and finally the angular velocities $p$, $q$, $r$.

The 3D trajectory in Fig. 6 represents a straight line as the angular velocity is null while the linear velocity is constant. The yaw angle is constant. This 3D trajectory in Fig. 7 represents a part of a helix with constant curvature and torsion. The yaw angle has a linear variation while the angular and linear velocities are constant. As can be seen in Fig. 8, after a transient phenomenon, in case #3 the yaw angle has a linear variation and the path tends to a classical helix with

Table 1. Five cases for a normalized simulation time = 1.

| Case | 1 | 2 | 3 | 4 | 5 |
|---|---|---|---|---|---|
| $\phi_0$ | 0 | $\pi/12$ | $\pi/12$ | $\pi/12$ | $\pi/12$ |
| $\dot{\phi}_0$ | 0 | 0 | 0 | 0.1 | 0.1 |
| $\theta_0$ | 0 | $\pi/6$ | $\pi/6$ | $\pi/6$ | $\pi/6$ |
| $\dot{\theta}_0$ | 0 | 0 | 0.1 | 0 | 0.1 |
| $u$ | 1 | 1 | 1 | 1 | 1 |
| $\dot{u}$ | 0 | 0 | 0 | 0 | 0.1 |
| Figure | 6 | 7 | 8 | 9 | 10 |

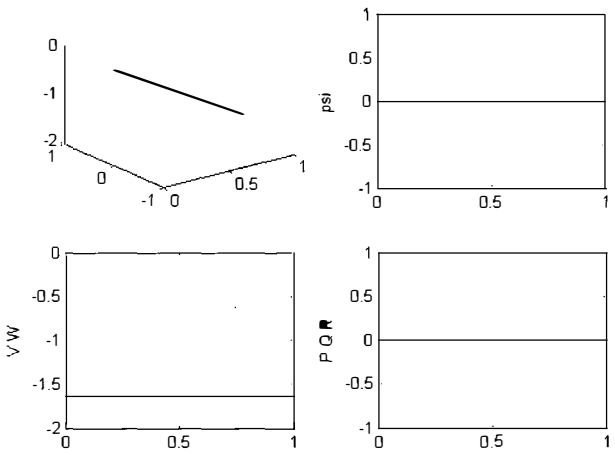


Fig. 6. Case #1.

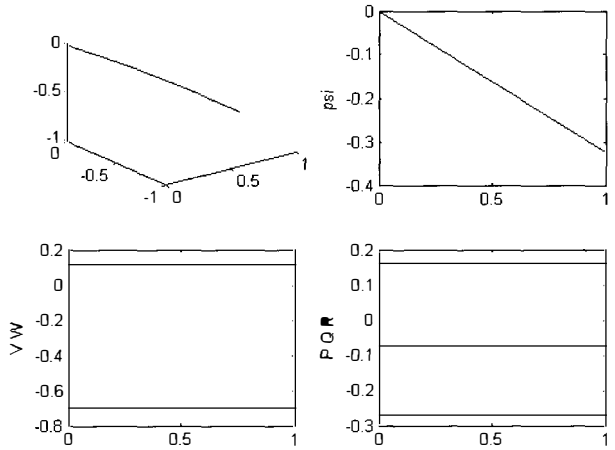


Fig. 7. Case # 2.

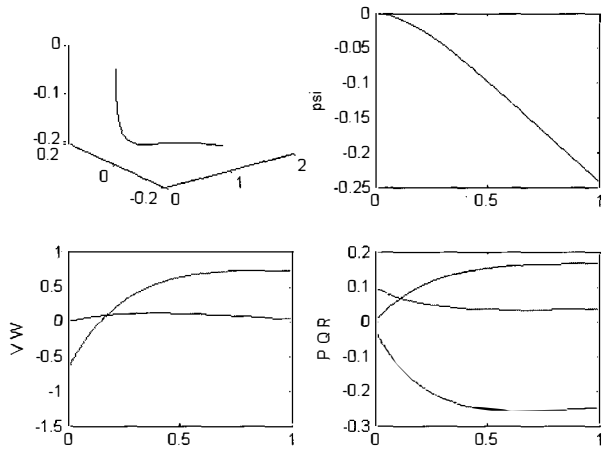


Fig. 8. Case # 3.

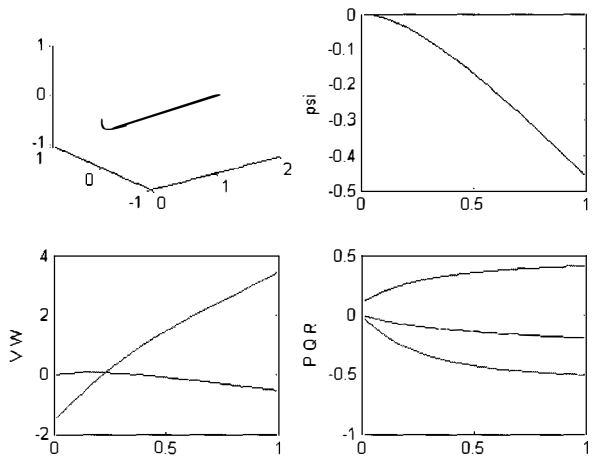


Fig. 9. Case # 4.

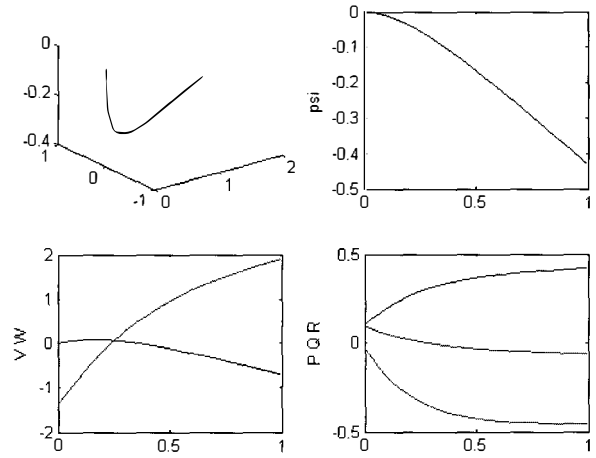


Fig. 10. Case # 5.

constant curvature and torsion.

In case #4, Fig. 9 shows that the angular and linear velocities have a slight nonlinear variation. After a certain time, they tend to have permanent values. For case #5, when the derivative of the longitudinal velocity is non zero, the nonlinear phenomenon is amplified in Fig. 10.

## 6. CONCLUSION

This paper addresses the problem of characterizing continuous paths in 3D, taking into account the under-actuation. Three differential algebraic equations must be solved as there is six degrees of freedom and three inputs. The constraints on the yaw angle is in the form of a generalized logistic equation while the others are differential algebraic equations in v and w, when the variations of the longitudinal velocity u, and the pitch and roll angles $\theta$, $\phi$ are imposed. The role of the trajectory generator is to generate a feasible time trajectory for the UAV. Once the path has been calculated in the Earth fixed frame, motion must be investigated and reference trajectories determined taking into account actuators constraints. This is the subject of our actual research. This method can be suitable for precise flight path tracking tasks, such as in landing approach. As a further application of the trajectory determination, the prediction of a cone of feasible future positions can be determined to evaluate the influence of the different kinematic parameters on the future flight path.

This methodology can be applied to other types of UAV, taking into account their characteristics. For fixed wing aircraft or helicopter, the added mass and inertia are neglected.

## REFERENCES

[1] Y. Bestaoui, "On line reference trajectory definition with joint torque and velocity constraints," *International Journal of Robotics Research*, vol. 11, no. 1, pp. 75-85, 1992.

[2] Y. Bestaoui, P. Plédel, and M. Gautier, "Motion generation in Cartesian space for industrial robots with actuators limitations," *Proc. of IEEE Congress on Decision and Control*, Kobe, Japan, pp. 863- 868, 1996.

[3] R. J. Murray, S. Sastry, and Z. Li, *A Mathematical Introduction to Robotic Manipulation*, CRC Press, 1994.

[4] K. G. Shin and N. D. McKay, "Minimum time control for robotic manipulators with geometric path constraints," *IEEE Trans. on Automatic Control*, vol. 30, pp. 531-541, 1985.

[5] P. Thomasson "Equations of motion of a vehicle in a moving fluid," *Journal of Aircraft*, vol. 37, no. 4, pp. 631-639, 2000.

[6] P. Plédel and Y. Bestaoui, "Actuator constraints in optimal motion planning of manipulators," *Proc. of IEEE International Conference on Robotics and Automation*, Nagoya, Japan, pp. 2427-2432, 1995.

[7] C. Belta and V. Kumar, "An SVD based projection method for interpolation on SE(3)," *IEEE Trans. on Robotics and Automation*, vol. 18, no. 3, pp. 334-345, 2002.

[8] E. Anderson, *Constrained Extremal Trajectories and UAV Path Planning*, M.S. thesis, Brigham Young University, 2002.

[9] G. Avanzini, "Frenet based algorithm for trajectory prediction," *AIAA J. of Guidance, Control and Dynamics*, vol. 27, no. 1, pp. 127-135, 2004.

[10] R. Beard, T. McLain, M. Goodrich, and E. Anderson, "Coordinated target assignment and intercept for unmanned air vehicles," *IEEE Trans. on Robotics and Automation*, vol. 18, no. 6, pp. 911-922, 2002.

[11] Y. Bestaoui, S. Hima, and C. Sentouh, "Motion planning of a fully actuated unmanned air

vehicle," *Proc. of AIAA Conference on Navigation, Guidance and Control*, Austin, Texas, Aug. 2003.

[12] E. Frazzoli, *Robust Hybrid Control for Autonomous Vehicle Motion Planning*, Ph.D. Thesis, MIT, Cambridge, Ma, 2001.

[13] S. Hima and Y. Bestaoui, "Motion generation on trim trajectories for an autonomous under-actuated airship," *Proc. of the 4th International Airship conference*, Cambridge, England, July 2002.

[14] S. Hima and Y. Bestaoui, "Time optimal paths for lateral navigation of an autonomous underactuated airship," *Proc. of AIAA Conference on Navigation, Guidance and Control*, Austin, Texas, Aug. 2003.

[15] R. Olfati-Saber, *Nonlinear Control of Under-actuated Mechanical Systems with Application to Robotics and Aerospace Vehicles*, Ph.D. Thesis, MIT, Cambridge, Ma, February 2001.

[16] Z. Shiller and H. H. Lu, "Computation of path constrained time optimal motions with dynamic singularities," *ASME Dynamic Systems, Measurement and Control*, vol. 114, pp. 34-40, 1992.

[17] H. J. Sussmann, "Shortest 3 dimensional paths with a prescribed curvature bound," *Proc. of the 34th IEEE Conf. on Decision and Control,* New Orleans, pp. 3306-3312, 1995.

[18] Y. Bestaoui and S. Hima, "Some insights in path planning of small autonomous blimps," *Archives of Control Sciences*, vol. 11, pp. 139-166, 2001.

[19] T. Das, R. Mukherjee, and J. Cameron, "Optimal trajectory planning for hot air balloons in linear wind fields," *AIAA Journal of Guidance, Control and Dynamics*, vol. 26, no. 3, pp. 416-424, 2003.

[20] Y. Bestaoui and T. Hamel, "Dynamic modeling of small autonomous blimps," *Proc. of Methods and Models in Automation and Robotics*, Miedzyzdroje, Poland, pp. 579-584, 2000.

[21] T. Fossen, *Guidance and Control of Ocean Vehicle*, J. Wiley Press, 1996.

[22] G. A. Khoury, J. D. Gillet, eds., *Airship Technology*, Cambrigde University Press, 1999.

[23] N. Azouz, Y. Bestaoui, and O. Lemaître, "Dynamic analysis of airships with small deformations," *Proc. of the 3rd IEEE Workshop on Robot Motion and Control,* Bukowy-Dworek, pp. 209-215, November 2002.

[24] G. G. Galanis and P. K. Palamides, "Global positive solutions of a generalized logistic equation with bounded and unbounded coefficients," *Electronic Journal of Differential Equations*, vol. 2003, no. 119, pp. 1-13, 2003.

[25] R. Grimshaw, *Non Linear Ordinary Differential Equations*, CRC Press, 1993.

[26] D. Jiang, J. Wei, and B. Zhang, "Positive periodic solutions of functional differential equations and population models," *Electronic Journal of Differential Equations*, vol. 2002, no. 71, pp. 1-13, 2002.

[27] M. N. Nkashama, "Dynamics of logistic equations with non autonomous bounded coefficients," *Electronic Journal of Differential Equations*, vol. 2000, no. 2, pp.1-8, 2000.